A regional registration technique for automated interval change analysis of breast lesions on mammograms

S. Sanjay-Gopal, Heang-Ping Chan,[a)] Todd Wilson, Mark Helvie, Nicholas Petrick, and Berkman Sahiner
Department of Radiology, University of Michigan, Ann Arbor, Michigan 48109-0030

(Received 11 November 1998; accepted for publication 13 September 1999)

Analysis of interval change is a useful technique for detection of abnormalities in mammographic interpretation. Interval change analysis is routinely used by radiologists and its importance is well-established in clinical practice. As a first step to develop a computerized method for interval change analysis on mammograms, we are developing an automated regional registration technique to identify corresponding lesions on temporal pairs of mammograms. In this technique, the breast is first segmented from the background on the current and previous mammograms. The breast edges are then aligned using a global alignment procedure based on the mutual information between the breast regions in the two images. Using the nipple location and the breast centroid estimated independently on both mammograms, a polar coordinate system is defined for each image. The polar coordinate of the centroid of a lesion detected on the most recent mammogram is used to obtain an initial estimate of its location on the previous mammogram and to define a fan-shaped search region. A search for a matching structure to the lesion is then performed in the fan-shaped region on the previous mammogram to obtain a final estimate of its location. In this study, a quantitative evaluation of registration accuracy has been performed with a data set of 74 temporal pairs of mammograms and ground-truth correspondence information provided by an experienced radiologist. The most recent mammogram of each temporal pair exhibited a biopsy-proven mass. We have investigated the usefulness of correlation and mutual information as search criteria for determining corresponding regions on mammograms for the biopsy-proven masses. In 85% of the cases (63/74 temporal pairs) the region on the previous mammogram that corresponded to the mass on the current mammogram was correctly identified. The region centroid identified by the registration technique had an average distance of 2.8 ± 1.9 mm from the centroid of the radiologist-identified region. These results indicate that our new registration technique may be useful for establishing correspondence between structures on current and previous mammograms. Once such a correspondence is established an interval change analysis could be performed to aid in both detection as well as classification of abnormal breast densities. [S0094-2405(99)00612-4]

Key words: image registration, computer-aided diagnosis, computer vision, interval change, breast cancer

I. INTRODUCTION

Mammography is currently the most effective method for early breast cancer detection.[1,2] A variety of computer-aided diagnosis (CAD) techniques have recently been developed to detect mammographic abnormalities and to distinguish between malignant and benign lesions.[3–8] Knowledge from diverse areas such as signal and image processing, pattern recognition, computer vision, artificial intelligence, and neural networks has been used to develop algorithms to be implemented within a CAD scheme. Varying degrees of success for these approaches have been reported in the literature. One common feature of most of these CAD techniques is that they use a single mammogram for analysis. However, some malignancies may only manifest as a new density on mammograms without associated calcifications or masses, others distinguish themselves from benign lesions only by their relatively rapid changes in sizes. Therefore, radiologists routinely use several mammographic views along with mammograms obtained in previous years for detecting and evaluating breast lesions and for identifying interval changes. The importance of interval change analysis in mammographic interpretation has been established in clinical practice.[9,10] It can be expected that analysis of changes in mammographic features between current and previous mammograms of the patient will also be an important component of a CAD system for both the detection and the classification tasks. The ability for automated analysis of interval changes would further the ability of CAD to offer an objective second opinion. This improvement, in turn, could increase the positive predictive value of mammography, reduce the number of benign biopsies, and hence reduce both cost and patient morbidity.

While a number of CAD schemes use only a single mammogram, the simultaneous use of more than one mammogram has been under investigation for some time. Several researchers have used views of the contra-lateral breast for detecting masses and developing densities. For instance, Yin *et al.*[11,12] have utilized architectural asymmetry between the right and left breasts to detect masses. While it is widely accepted that interval changes in mammographic features are very useful for both detection and classification of breast abnormalities, the development of CAD techniques to use this information has achieved limited success.[13–18] Sallam and Bowyer[13] have proposed a warping technique for mammogram registration. They manually obtained control points and calculated a mapping function for mapping each point on the current mammogram to a point on the previous mammogram. The mapping function was obtained based on local affine transformations, as well as interpolation and surface fitting techniques. A drawback of this technique is the need for manual demarcation of control points. Brzakovic *et al.*[14] have investigated a three-step method for comparison of most recent and previous mammograms. They first registered two mammograms using the method of principal axis, and partitioned the current mammogram using a hierarchical region-growing technique. The breast regions in the two mammograms were aligned with respect to each other by means of translation, rotation, and scaling. Although the technique was evaluated on a total of 64 images obtained from eight cases, this work mainly aimed toward detecting cancerous changes in breast tissue and, therefore, no quantitative analysis of registration accuracy was presented. Vujovic and co-workers[15,16] have proposed a multiple-control-point technique for mammogram registration. They first determined several control points independently on the current and previous mammograms based on the intersection points of prominent anatomical structures in the breast. A correspondence between these control points was established based on a search in a local neighborhood around the control point of interest. In a more recent publication,[17] they have evaluated their approach for establishing the correspondence between control points extracted from two mammograms using 29 temporal image pairs, and presented a qualitative evaluation based on an observer study. They have demonstrated that 91% of 103 computer-matched control points were in agreement with those matched by a radiologist. An important assumption of their work was that the distances between the control points did not change significantly between the two mammograms. However, this assumption is not necessarily a valid one. Variations in compression could potentially cause a large variation in the relative distances between the control points. Furthermore, the control points representing the intersections of elongated structures do not always have correspondences on the two mammograms. Most of these points are two-dimensional projection image of structures at different depths of an elastic and compressible three-dimensional breast. The projected intersection points can thus vary from image to image and are not invariant lankmarks. As noted by the authors, the potential control points are not points that are naturally selected by a radiologist when examining mammograms. Hence, the significance of these points is debatable.

An important factor that may limit the success of the above-mentioned techniques is that the extraction of any meaningful information from previous mammograms first requires a common frame of reference between the current and previous mammograms. Several complicating factors confound obtaining such a frame of reference. These factors include differences in breast compression and positioning between the current and previous mammograms, differences in the imaging technique between the two examinations, and changes in breast structure, size, and tissue density between the two images with patient age. As a result, the mammographic appearance of breast tissue on the current and previous mammograms of the same patient may vary considerably. Although these variabilities have not been quantified experimentally, they can be observed easily from most mammograms. Conventional registration techniques work well for applications involving rigid objects. Because of the elasticity of the breast tissue, the absence of obvious landmarks, and the large variability in the relative positions of the breast tissues projected onto the mammogram from one examination to the other, these techniques may not be optimal for registration of breast images.

In mammographic interpretation, a radiologist routinely compares the current mammogram with previous mammograms (if available) of the same view in order to detect changes in mammographic features. For example, if a mass is detected in the current mammogram, the radiologist searches for that mass in the previous mammogram to determine if this is a new or developing density. If the corresponding mass is found on the previous mammogram, then the radiologist compares the current and previous mass size and estimates if the mass has increased in size. To facilitate these comparisons, we plan to develop automated methods to detect the interval changes as a part of a computer-aided diagnostic system. As a first step, we have developed a novel method for automatic registration of lesions on temporal pairs of mammograms. In our approach, the computer emulates the search method used by many radiologists for finding corresponding structures on mammograms. The method aims at registering a small region containing a suspected mass on the most recent mammogram of the patient with one on a mammogram obtained from a previous year. Our regional registration technique involves three steps: (1) identification of a suspicious structure on the most recent mammogram, (2) initial estimation of the location on a previous mammogram of the region corresponding to the suspicious structure and the definition of a search region which encloses the object of interest on the previous mammogram, and (3) accurate identification of the location of the matched object within the search region. After the two matched lesions are identified, their characteristic features can be automatically extracted and interval changes estimated. In the present study, we focused on the development and the evaluation of the regional registration technique, rather than to solve the entire interval change analysis problem. The subsequent steps in the interval change analysis are beyond the scope of this study.

In the following sections we will provide a detailed description of our regional registration technique for temporal registration of mammograms and the results of a quantitative evaluation using a data set of 74 temporal image pairs. Although we evaluated a semiautomated version of the tech-

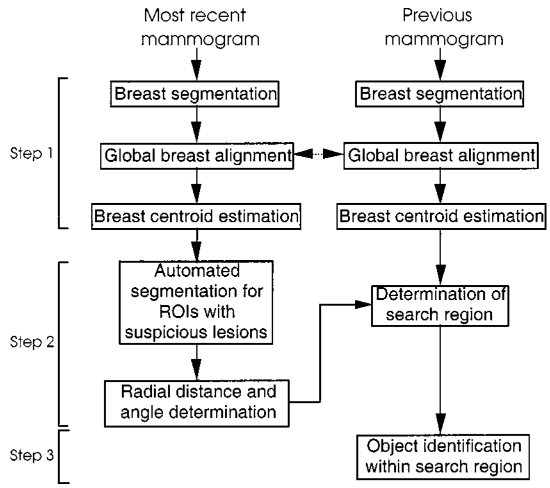

FIG. 1. Regional registration technique for determining an object on the previous mammogram which corresponds to a suspicious object on the most recent or current mammogram.

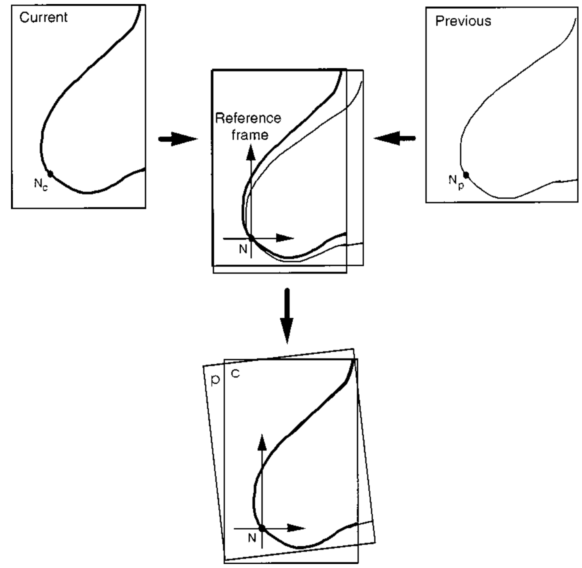

FIG. 2. Global breast alignment based on the mutual information between the two breast regions. N_c—nipple location in current mammogram, N_p—nipple location in previous mammogram, N—nipple location for both current and previous mammograms after translating them to the common frame of reference. The previous mammogram is rotated until the mutual information between the two mammograms is maximized.

nique in this preliminary study, it can be fully automated by incorporating a nipple detection step so that no user interaction will be required.

II. MATERIALS AND METHODS

A. Regional registration and mammogram correspondence

As the term indicates, regional registration is a local rather than a global registration technique. It is a multistep procedure and utilizes computer-detected objects in the most recent (hereafter termed current) mammogram. In the context of this paper, a current mammogram is either the latest mammogram of the patient, or the latest mammogram before biopsy. The detected objects could be either true masses (benign or malignant) or false positives (normal breast structures). Regional registration then finds a matching object on a previous mammogram. The three major steps in regional registration are illustrated in Fig. 1 and details of the technique are described below.

In the first step of regional registration, the breast region is segmented from the background on both the current and the previous mammograms. For this purpose we have used a breast boundary detection algorithm previously developed in our laboratory.[19,20] This algorithm could successfully track the breast boundaries in over 90% of the 1000 mammograms in a previous study. It performed reliably on all the images in our database. After extracting the breast border from the mammogram, the location of the nipple is estimated on both the current and the previous mammograms. Any automated method[21,22] can be used for finding the nipple location. However, in this study, the nipple location was manually identified by a radiologist for all images in our data set. The breast border and the nipple location now form the basis of a global breast alignment (GBA) procedure illustrated in Fig. 2. Since the sizes and the orientations of the two images could vary between the current and previous mammograms, a common frame of reference is needed. The GBA procedure has been devised specifically to provide such a frame of reference. We first define a new frame of reference with the nipple location on the current mammogram (N_c) as the origin. The previous mammogram is translated so that its nipple location (N_p) aligns with the origin in the common frame of reference as shown in Fig. 2. Using the origin as the pivot point, we rotate the previous mammogram to align the breast regions in the two images.

We have evaluated two different methods for estimation of the optimum rotation angle. The first method is based on maximization of the overlap area, and the second method is based on maximization of the mutual information (MI)[23,24] between the two segmented breast regions. To determine the MI, we first rescale the breast portion of both mammograms to a 0–255 gray scale. For a given rotation angle θ, the two-dimensional (2D) histogram $h_\theta(i,j)$ of the gray levels for the corresponding pixels on the current mammogram and the previous mammogram is constructed. Here i refers to the gray level on the current mammogram and j refers to the gray level on the previous mammogram rotated by an angle θ. The probability density of the gray scale co-occurrences is estimated from the 2D histogram as

$$f_\theta(i,j)=\frac{h_\theta(i,j)}{\Sigma_{m,n}h_\theta(m,n)}, \tag{1}$$

where $0\leqslant i,j\leqslant 255$, $0\leqslant m,n\leqslant 255$. The mutual information (MI_θ) between the two images for a specific rotation angle θ is computed as

$$\mathrm{MI}_\theta=\sum_{i,j} f_\theta(i,j)*\log_2\left\{\frac{f_\theta(i,j)}{\Sigma_m f_\theta(i,m)\Sigma_n f_\theta(n,j)}\right\}. \tag{2}$$

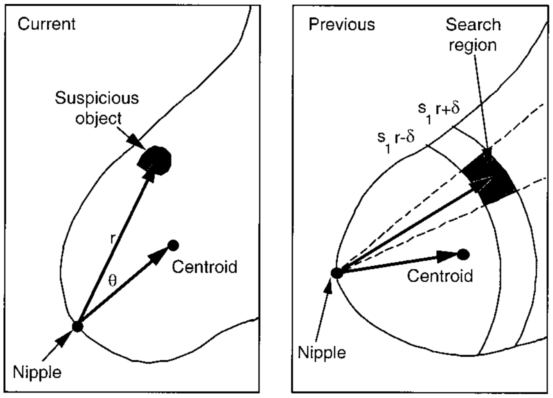

FIG. 3. Polar coordinate system defined using the nipple location and the nipple–centroid axis. The search region for finding a matching object on the previous mammogram is shown as the shaded region.

The above-mentioned procedure is repeated for several rotation angles and the angle $\theta_{\max}$ which provides the maximum mutual information is chosen for global breast alignment of the previous mammogram and the current mammogram. Note that while the area overlap method for GBA uses the binary image after segmentation, the MI-based method uses the original gray scale image. The effects of the two methods on the accuracy of regional registration will be discussed later in Sec. IV. Once the two images are aligned in the common frame of reference, the centroid of the breast region is estimated, and the nipple–centroid axis is defined for both mammograms. For comparison we also show in Sec. III regional registration results based on computing the centroids of the two breast regions without global breast alignment. The nipple–centroid axis forms the basis for the second step of regional registration.

In the second step, suspicious regions are automatically segmented from the breast region on the current mammogram. This can be accomplished by using a density-weighted contrast enhancement (DWCE) technique[25] previously developed in our laboratory. While the use of the DWCE technique is not critical for regional registration, it does help automate the entire procedure. Alternatively, a radiologist can manually identify a suspicious object or a region of interest on the current mammogram and the regional registration technique can be used to identify a corresponding region on the previous mammogram. Once suspicious objects have been identified on the current mammogram, the centroid of each object is estimated. A polar coordinate system is then defined using the nipple as the origin and the nipple–centroid axis as the 0° axis on both images. This is illustrated in Fig. 3. The location of the centroid of a suspicious object on the current mammogram is determined as (r,θ). We then compute two scale factors—the radial scale factor s_1 and the angular scale factor s_2. These scale factors have been devised to provide a first-order correction for factors such as breast compression differences between the current and previous mammograms, differences in image magnification and size, and changes in overall breast shape between the two images. The radial scale factor s_1 is estimated as the ratio of the nipple–centroid distances on the previous and current images. The angular scale factor s_2 is estimated as the ratio of the angular width of the breast on the previous image at radius $s_1 r$ to that on the current image at radius r. The initial estimate of the corresponding location of the suspicious object on the previous mammogram is then obtained as $(s_1 r, s_2\theta)$.

Using the initial estimate of the centroid of the object on the previous mammogram, we can define a fan-shaped search region bounded by $s_1 r \pm \delta$ and $s_2\theta \pm \epsilon$ as illustrated in Fig. 3. The object found on the current mammogram is then used as a template to search for a matching object in the search region on the previous mammogram. The size of the search region (defined by δ and ϵ) depends on the variability between mammograms obtained from one examination to the other. Since it is difficult to predict the variability of an elastic and deformable object such as the breast by any analytical method, we have determined this variability experimentally from the mammograms in our data set. The variation in compression can cause a change in the relative locations of various breast structures on these images as well as a rotation of the breast boundary with respect to the fixed image coordinates. By relating the position of a breast structure to the corresponding nipple–centroid axis, and by performing a search in the corresponding search region, we can reduce the effect of this variability. In this study we have estimated the size of the search region required to enclose all corresponding objects on the previous mammogram using ground truth objects identified on the previous mammograms by a radiologist. The distance of the initial estimate of the center of the search region from the centroid of the ground truth object was also estimated.

The third and final step in the regional registration procedure involves a systematic search to identify a corresponding structure within the fan-shaped search region on the previous mammogram. In this study we have evaluated two different search criteria. The first criterion is based on gray scale template matching. A rectangular gray scale template centered on the mass centroid is extracted from the current mammogram. The choice of the size of the template region can affect the accuracy of the registration technique. The minimum required size of a rectangular template is, of course, a rectangular region which encloses the mass exactly. However, one can also include a small portion of the background region in the template. We have analyzed the performance of our algorithm using two different sizes for this template. The first includes a 1-pixel-wide background region all around the boundary of the suspicious object while the second includes a 5-pixel-wide background region. For each pixel (i,j) in the fan-shaped region on the previous mammogram, a region of interest (ROI) centered on the pixel and of the same size as the mass template is extracted. We denote the (m,n)th pixel in the gray scale template extracted from the current mammogram as $p(m,n)$ and that from the ROI obtained from the fan-shaped region as $q_{i,j}(m,n)$. A correlation measure defined as

$$C_{i,j}=\frac{\Sigma_{m,n}(p(m,n)-\overline{p})(q_{i,j}(m,n)-\overline{q})}{\sqrt{(\Sigma_{m,n}(p(m,n)-\overline{p})^2)(\Sigma_{m,n}(q_{i,j}(m,n)-\overline{q})^2)}} \quad (3)$$

is then obtained for each pixel (i,j) within the search region on the previous mammogram. Here the summation is performed over the mass template, and $\overline{p}$ and $\overline{q}$ denote the average pixel values in the template and ROI, respectively. The correlation values in the search region are then smoothed by a 3×3 averaging kernel to reduce fluctuations. The final estimate of the location of the mass centroid on the previous mammogram is obtained as the location corresponding to maximum correlation. The second search criterion is based on maximizing the mutual information between the mass template and the ROI extracted from within the search region. The MI approach is similar to that described earlier for alignment of the breast regions, except that the regions to be matched are limited to the size of the mass template.

Once a corresponding structure is found on the previous mammogram for a suspicious object on the current mammogram, it can be used for an interval change analysis within a CAD scheme, as we have shown in an independent study.[26] If the search procedure in the fan-shaped region does not yield a corresponding region, then the suspicious object on the current mammogram can be considered as a newly developed density. Objects for which no corresponding object can be found on the previous mammogram can be analyzed with methods designed for single images in an overall CAD scheme. Note that in this study the search techniques are structured in a way to always determine a matching object. Search criteria to identify new densities will be developed in future studies.

B. Image acquisition and data set

The data set for this study consisted of 127 images obtained from the files of 34 patients who had undergone biopsy at the University of Michigan. From these 127 mammograms, 74 temporal pairs of images were obtained. The current mammogram of each temporal pair exhibited a biopsy-proven mass. All previous mammograms in the 74 temporal pairs contained a mass, a structure, or a density which the radiologist could match to the mass detected in the corresponding current image. Since some patient files contained a sequence of mammograms over three years, the number of temporal pairs was larger than half the number of images. The 74 temporal image pairs were comprised of 43 cranio-caudal views and 31 mediolateral-oblique views.

The mammograms of 20 temporal pairs were digitized with a LUMISYS DIS-1000 laser scanner at a pixel resolution of 0.1 mm×0.1 mm and with 12 bit resolution. The digitizer was calibrated so that the gray values were linearly and inversely proportional to the optical density (OD) within the range of 0.1–2.8 OD units, with a slope of −0.001 OD/pixel value. Outside this range, the slope of the calibration curve decreased gradually. The OD range of this digitizer was 0–3.5. The mammograms of the remaining 54 temporal pairs were digitized with a LUMISCAN 85 laser scanner at a pixel resolution of 0.05 mm×0.05 mm and with 12 bit resolution. This digitizer was calibrated so that the gray values were linearly and inversely proportional to the OD within the range 0–4 OD units, with a slope of −0.001 OD/pixel value. All images were subsequently reduced to 0.8 mm resolution by averaging adjacent 8×8 pixels (20 pairs) or 16×16 pixels (54 pairs). Since the same digitizer was used for digitizing all films of the same case, the differences in the digitizers would have no effect on the analysis of each image pair. Given the small differences between the two laser digitizers and the large differences in the imaging technique and in the breast appearance from one case to another, it could be expected that the use of cases collected with the two different digitizers would not affect the evaluation of the registration technique.

While the regional registration technique can be used for determining a corresponding structure or region for any structure (both false positives and masses) in the breast, in this study we have analyzed its accuracy on biopsy-proven masses alone. The location of the mass on the current mammogram was identified by an MQSA-certified radiologist experienced in breast imaging. The radiologist manually identified the corresponding region on the previous mammogram and the nipple location on both the current and the previous mammograms using an interactive image analysis tool on a UNIX workstation. For each current mammogram, the boundary of the mass was manually delineated by the radiologist using an image display program developed in our laboratory. A bounding box enclosing the corresponding object on the previous mammogram was provided by the radiologist for each of the masses. Each mass as well as the corresponding structure on the previous mammogram was rated for its visibility on a scale of 1–10, where the rating of

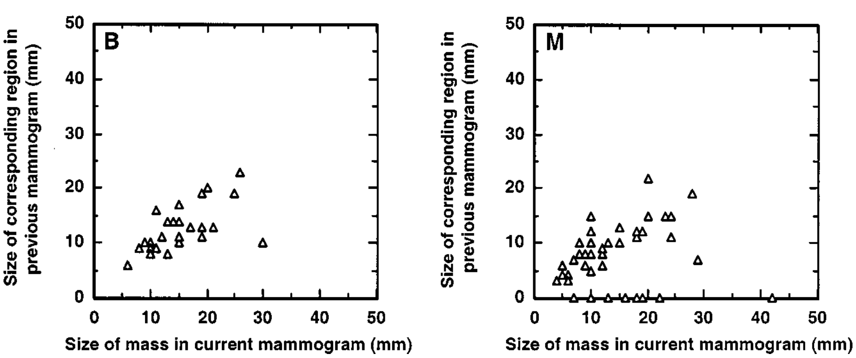

FIG. 4. Distribution of the size of the mass on the current mammogram with respect to the size of the corresponding structure on the previous mammogram as estimated by an experienced breast radiologist for benign (B) and malignant (M) cases in the data set.

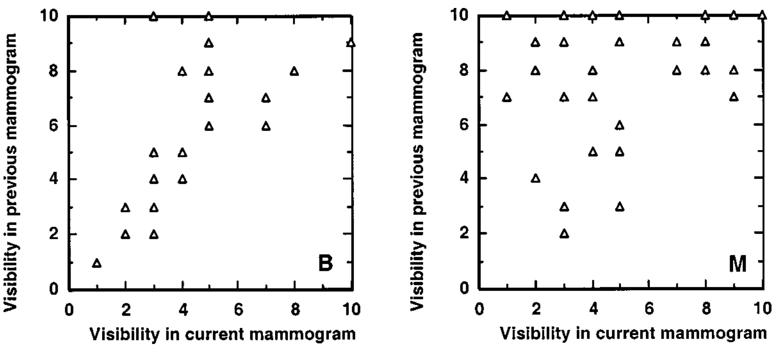

FIG. 5. Distribution of the visibility of the mass on the current mammogram with respect to the visibility of a corresponding structure on the previous mammogram as rated by an experienced breast radiologist for benign (B) and malignant (M) cases. In this rating scale the visibility of the masses decreases from 1 to 10 with 10 being the least visible. The total number of points in these two graphs is less than the total number of mammogram pairs in our database, because mammogram pairs with the same rating appear as a single point.

1 corresponded to the most visible category. The size of the mass on the current mammogram as well as the size of the corresponding structure on the previous mammogram was also provided by the radiologist. For previous mammograms on which the radiologist could not identify a distinct mass, the ''mass'' size was given a size of 0 mm. The parenchymal density was rated based on the BIRADS lexicon. The distributions of the size and visibility ratings for benign and malignant cases in this data set are shown in Figs. 4 and 5.

C. Evaluation of registration accuracy

The bounding box enclosing the corresponding object on the previous mammogram provided by the radiologist was used as the ''ground truth'' to evaluate the accuracy of the regional registration technique. We have used two different measures for assessing registration accuracy. The first measure quantifies whether the corresponding region is correctly identified by the registration algorithm. This measure is computed simply as the number of cases in which the estimated centroid location of the mass on the previous mammogram is inside the bounding box provided by the radiologist. The second measure quantifies the error in the estimate of the corresponding region on the previous mammogram and is defined as the Euclidean distance between the estimated centroid of the corresponding region and the center of the bounding box provided by the radiologist. Together these two measures answer the questions: (a) does regional registration work? (b) how well does the technique perform in matching structures between the current and previous mammograms? In Sec. III we provide the results of regional registration with and without global breast alignment and using both correlation and mutual information as the search criterion in step 3.

III. RESULTS

To provide the reader with a qualitative idea of algorithm performance we first illustrate the intermediate results at various stages of the algorithm. Then the results of each of the three steps of the algorithm are presented with an analysis of the dependence of the performance on various algorithm parameters. Also presented is an analysis of the accuracy of regional registration using the error measures defined in Sec. II C. In the following sections, the term ''initial estimate'' refers to the estimate of the center of the search region in step 2 of regional registration. The term ''final estimate'' refers to the outcome of the search procedure adopted in step 3 and represents the overall result of regional registration.

A. Intermediate results of regional registration

Figures 6–8 show an example of the intermediate and final results of applying the regional registration technique to a temporal pair of mammograms. The original digitized mammograms—current and previous—with the automati-

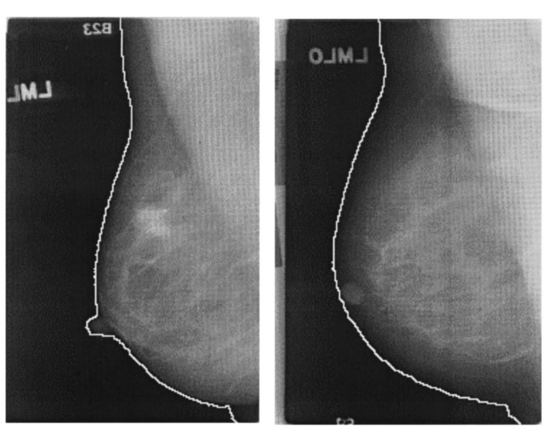

FIG. 6. Left—most recent or current mammogram. Right—previous mammogram. The breast images are superimposed with the breast borders detected by a breast boundary tracking algorithm.

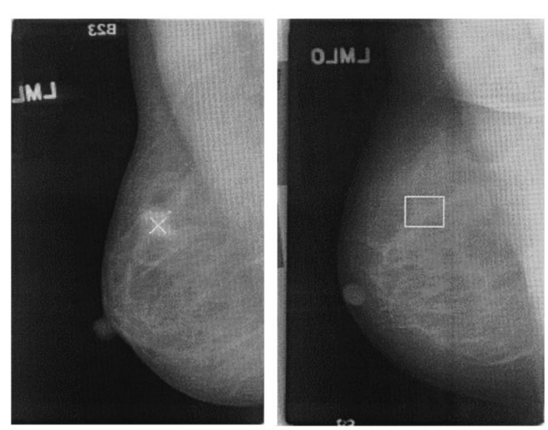

FIG. 7. Left—location of the mass on the current mammogram. Right—radiologist-identified region on previous mammogram corresponding to the mass on the current mammogram.

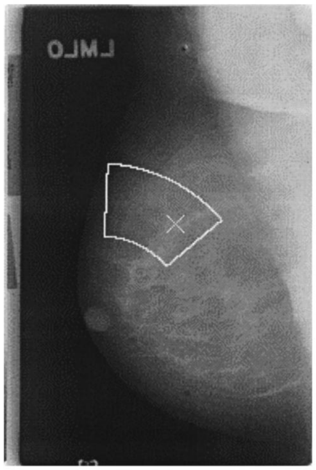

FIG. 8. The fan-shaped search region on the previous mammogram. The initial computer estimate of the centroid location of the region corresponding to the mass is at the center of the search region. The final estimate of the centroid of the corresponding region (indicated by *X*) is obtained by using the correlation criterion within the fan-shaped search region.

cally tracked breast boundaries superimposed, are shown in Fig. 6. The location of the mass on the current mammogram is shown in Fig. 7 along with the corresponding radiologist-identified region on the previous mammogram. Figure 8 shows the fan-shaped search region on the previous mammogram estimated in step 2 of regional registration. The initial estimate is at the center of this search region which is to be used in step 3 for localization of the corresponding mass. The centroid location of the corresponding object estimated by the algorithm using the correlation measure as the search criterion is also shown in Fig. 8.

B. Initial estimates and search regions

Figure 9 shows histograms of the Euclidean distance between the initial estimate of the centroid location of the corresponding structure on the previous mammogram and the center of the bounding box provided by the radiologist. For the 74 temporal image pairs used in this data set, the average Euclidean distance error of the initial estimate was 10.5 mm (std. dev. 6.4 mm) without the GBA procedure and 9.8 mm (std. dev. 6.0 mm) with the GBA procedure. The overall accuracy was 46% in both cases, i.e., in 34 of the 74 temporal image pairs the initial estimate was inside the ground-truth bounding box. Based on observation of the radial deviation errors and the angular deviation errors (defined in Sec. IV) in Figs. 10 and 11, a search region defined by $\epsilon = 0.35 + 5/r$ rad and $\delta = 20$ mm with GBA ($\delta = 25$ mm for no GBA), where r is the radial distance from the nipple, was used for the evaluation of the local search criteria used in step 3 of regional registration.

C. Local search criteria and final estimates

Figure 12 shows the histograms of the Euclidean distance errors of the final estimate of the corresponding structure using the correlation measure as the search criterion. Table I summarizes the results along with the average Euclidean distance errors and standard deviations using both the correlation and the mutual information search criteria and with and without the GBA procedure. The average Euclidean distance errors and deviations for the cases where the final estimate is inside the ground-truth region identified by the radiologist and the cases where it is outside are also listed separately. Regional registration incorporating the GBA procedure and using correlation as a search criterion has an accuracy of 85%. In 63 of the 74 temporal image pairs, the final estimate of the location of the corresponding region was inside the radiologist-identified ground-truth region. The use of mutual information as a search criterion yielded an accuracy of 74% (55 out of 74 temporal pairs). The average Euclidean distance error for regional registration incorporating GBA and correlation was 4.7 mm (std. dev. 5.8 mm) for all 74 temporal pairs and 2.8 mm (std. dev. 1.9 mm) in 85% (63/74) of the temporal pairs. Use of mutual information as a search criterion in step 3 results in values of 7.2 mm (std dev. 8.6 mm) and 3.0 mm (std. dev. 2.0 mm), respectively, for the same quantities.

IV. DISCUSSION

A. Initial estimates and search regions

From the histograms of Fig. 9, we observe that the use of the GBA procedure results only in a marginal improvement in the initial estimate, if the Euclidean distance error is the only measure considered. However, the GBA procedure has a significant effect in reducing the size of the search region required for regional registration. In order to compute the required sizes (δ and ϵ in Fig. 3) of the search region, we computed two quantities—the radial distance deviation and the angular deviation—using the initial estimate obtained from step 2 for the 74 temporal image pairs. The radial distance deviation is defined as the absolute difference between $s_1 r$ and r_c, where r_c is the radial distance of the center of the ground-truth region from the nipple location on the pre-

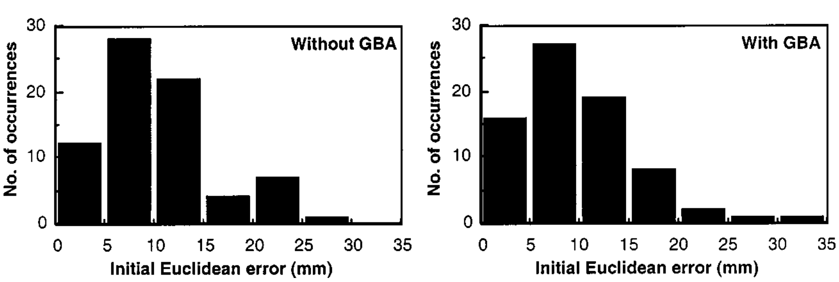

FIG. 9. Histograms of Euclidean distance between the initial estimate of the centroid location of the corresponding object and the center of the radiologist-identified object on the previous mammogram with and without GBA.

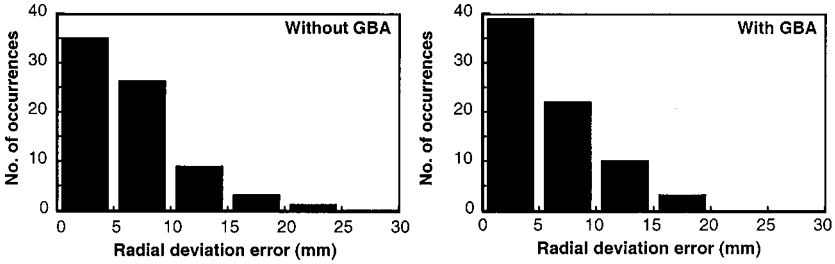

FIG. 10. Histograms of radial distance deviation between the initial estimate of the centroid location of the corresponding object and the center of the radiologist-identified object on the previous mammogram with and without GBA.

vious mammogram. The histograms of radial distance deviations for the 74 temporal image pairs with and without the GBA procedure are shown in Fig. 10. An important observation is that a δ value of 25 mm is needed to include the centers of the ground-truth structures if the GBA procedure is not used in step 1. The use of the GBA procedure results in a decrease in the value of δ to 20 mm. This decrease helps significantly increase the overall accuracy of the regional registration as discussed below.

In Fig. 11 the angular deviation of the initial estimate is plotted against the radial distance of the centers of the ground-truth regions on the previous mammogram. The angular deviation ϵ is defined as $s_2\theta-\theta_c$ where θ_c is the angle between the nipple-ground-truth center vector and the nipple-centroid axis. In an earlier study[27] using both false positives and masses, we have observed that the value of ϵ needed to include the center of the ground-truth region decreases with distance from the nipple, i.e., increases with distance from the chest wall. This may be attributed to the increased deformability of the breast tissue closer to the nipple compared to the tissue closer to the chest wall. This indicates that a possible approach to take into account this variability is to incorporate a variable ϵ, one which is inversely proportional to the radial distance r from the nipple. For the data set in this study, we have investigated several forms for this dependence all of which fit under the general model

$$\epsilon=\epsilon_{\mathrm{th}}+K/r.$$

Here ϵ_{th} and K are two constants which affect the form of the dependency. Based on our observation of the angular deviations for the entire data set of 74 temporal pairs we have chosen $\epsilon_{\mathrm{th}}=0.35$ rad and $K=5$ rad-mm. As can be seen from Fig. 11, with these values of ϵ_{th} and K, all of the centers of the ground-truth regions are within the search region. Therefore, a search region defined by $\epsilon=0.35+5/r$ rad, and $\delta=20$ mm (if GBA was applied) or $\delta=25$ mm (if GBA was not applied) was used for evaluation of the local search criteria used in step 3 of regional registration.

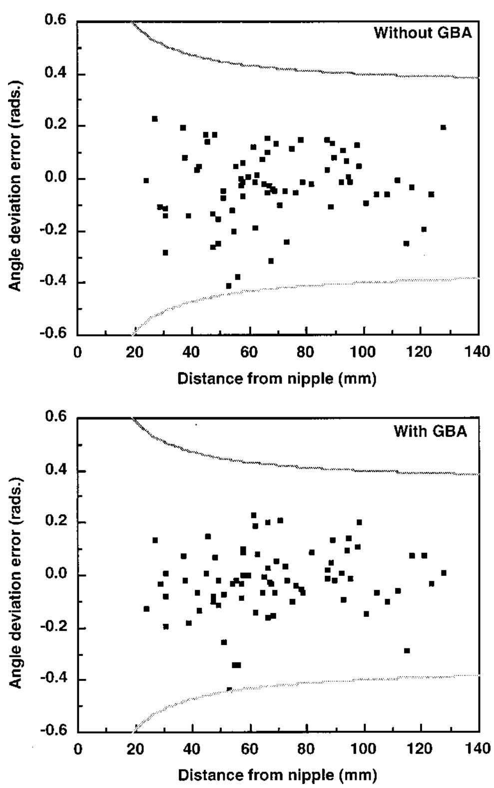

FIG. 11. Angular deviation between the initial estimate of the centroid location of the corresponding object and the center of the radiologist-identified object on the previous mammogram with and without GBA. Also shown are the bounding lines defined using $\epsilon=0.35+5/r$ rad.

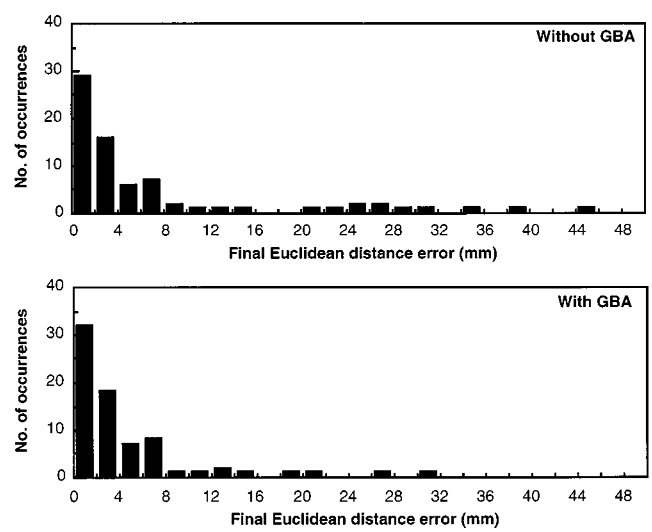

FIG. 12. Histograms of Euclidean distance error for corresponding regions estimated by regional registration using the correlation measure in step 3 with and without GBA. This error is defined as the Euclidean distance between the centroid location of the estimated corresponding region and the center of the radiologist-identified ground-truth corresponding region on the previous mammogram.

TABLE I. Accuracy of regional registration using correlation measure and mutual information measure in step 3 with and without global breast alignment (GBA) and using a 1-pixel-wide background region for the template from the current mammogram. Correct estimates are the cases where the estimated centroid location was within the bounding box of the radiologist-identified object location.

Method	Accuracy	Overall average error (mm)	Average error (mm) for correct estimates	Average error (mm) for incorrect estimates
Correlation without GBA	77% (57/74)	7.4±10.2	2.8±2.0	22.9±11.5
Mutual information without GBA	68% (50/74)	8.8±10.5	3.0±2.0	20.7±11.1
Correlation with GBA	85% (63/74)	4.7±5.8	2.8±1.9	15.7±8.3
Mutual information with GBA	74% (55/74)	7.2±8.6	3.0±2.0	19.4±8.9

B. Local search criteria and final estimates

We have evaluated the use of correlation and mutual information as the local search criteria. From Table I we observe that the GBA procedure results in a higher accuracy irrespective of the search criterion. While the use of mutual information as a search criterion performs reasonably well by itself (74% accuracy with an average error of 7.2 mm) the use of correlation measure was observed to result in more accurate registration. For the images in this data set, the correlation measure outperformed the mutual information measure irrespective of whether the breast centroids were computed with or without the GBA procedure.

A few observations on the 11 cases where the final estimate was outside the radiologist-identified ground-truth corresponding region are in order. In 7 of the 11 cases although the radiologist did provide a region corresponding to the mass on the current mammogram, the corresponding structure on the previous mammogram was very subtle (visibility rating 8 or higher) with indistinct boundaries. The radiologist could only estimate the region where the mass would develop rather than the mass itself, so the truth was uncertain. In one of the remaining 4 cases, the mass was an architectural distortion in the current mammogram. In a second (benign) case the mass shape had changed considerably. Upon consultation of the pathology report, the radiologist concluded that the mass was a benign cyst which had been aspirated in the previous year resulting in a substantial change in its shape. In the third case, the proximity of the mass to the chest wall resulted in it being incompletely imaged in the previous year compared to the current year. In such cases the correlation measure of a neighboring breast structure would tend to be higher than that of the corresponding structure. In the fourth case, an overlap of two vessels was identified as corresponding to the mass on the current mammogram while the region corresponding to the mass was observed to be extremely subtle. In almost all of the 11 cases the proximity of the corresponding region to a dense structure combined with the subtle nature of the structure on the previous mammogram render the correlation measure ineffective in establishing correspondence. However, in clinical practice, these masses will likely be categorized as a newly developed density. Criteria to distinguish a newly developed density will be investigated in further studies.

C. GBA: Area overlap vs mutual information

For the images used in this study, the result of the GBA procedure based on maximizing the area overlap between the breast regions in the two images of a temporal pair is comparable to that based on maximizing the mutual information. However, our observation is that the mutual information criterion is preferable to the area overlap criterion. The area overlap measure suffers from the drawback that if the breast region in one of the mammograms is uniformly smaller than that in the other, i.e., the breast edge in one is completely within the breast edge in the other, then there is no unique rotation angle at which the area overlap is maximized. Although the range of rotation angles over which local maxima of the area overlap occur is small, the resulting estimate of the rotation angle for GBA may be suboptimal. The use of mutual information, however, results in a single unique rotation angle at which MI is maximized. In any case, as discussed earlier, the use of the GBA procedure before computing the breast centroid results in a reduction in the size of the search region. A smaller search region reduces the likelihood that the mass template is matched to an incorrect structure and, therefore, increases the accuracy and reduces the Euclidean distance error.

D. Template size, scale factors, and computation times

The size of the background region in the gray scale template extracted from the current mammogram affects registration accuracy. For the 74 temporal pairs in this data set, the best performance was observed when a 1-pixel-wide background region was included all around the boundary of the mass template. A 5-pixel-wide background region resulted in a decrease in accuracy and an increase in the average Euclidean distance error. The accuracy progressively decreased and the Euclidean distance error increased with an increase in the size of the background region in the template. Figure 13 shows the distributions of the radial and angular scale factors for the images used in this study. The radial scale factor s_1 ranged from 0.94 to 1.05 for this data set. Use of s_1 reduced the size of the search area by decreasing the required value for δ. The angular scale factor s_2 was very close to 1 in all cases and did not seem to make any major difference for the images in this data set. On a final note the computation time required for regional registration incorporating correlation was on the average 2 s without GBA and 4 s with GBA on a UNIX workstation (DEC AlphaStation 600 series).

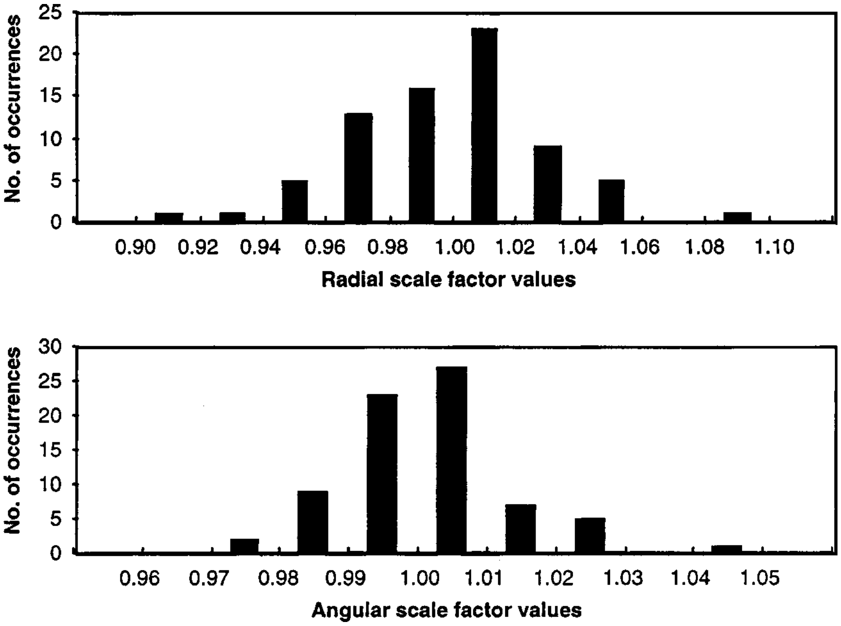

FIG. 13. Histograms of the radial scale factor and the angular scale factor for 74 temporal image pairs. The radial scale factor s_1 is estimated as the ratio of the nipple–centroid distances on the previous and current images. The angular scale factor s_2 is estimated as the ratio of the angular width of the breast on the previous image at radius $s_1 r$ to that on the current image at radius r.

V. CONCLUSIONS

Radiologists are interested in determining any local changes in breast tissue over time which may indicate a developing cancer. We have developed a novel regional registration technique for temporal registration of mammograms. This technique could become an important component of a CAD scheme for mammographic analysis. Unlike other techniques found in the literature, our regional registration technique does not depend on the identification of landmark structures or control points on the mammograms. It is based on a search technique that many radiologists use and has proven to be successful in mammographic interpretation. After corresponding objects are found, they can be analyzed for interval changes in a CAD scheme. Our preliminary results indicate that the regional registration technique is promising in identifying corresponding regions from temporal mammographic pairs. In 85% (63/74) of the cases the regional registration technique correctly identified the corresponding region in the previous mammogram. For these 63 cases, it is highly encouraging to note that the estimated location of the region corresponding to the mass in the current mammogram was less than 3 mm on the average from radiologist-identified corresponding locations.

Areas for future work include the development of an automated technique for identifying the nipple location on the mammograms, investigation of other local search criteria such as Fourier descriptors and shape-invariant moments to be used in the fan-shaped search region, adaptive methods for determining the size of the search region, criteria for identifying newly developed densities, application of regional registration to false positives as well as masses, and studies with a large data set to investigate the robustness of the regional registration technique. It may be noted that the regional registration technique may also be applicable to other related registration problems, such as the registration of left and right mammograms.

ACKNOWLEDGMENTS

This work is supported by a Career Development Award from the USAMRMC Grant No. DAMD 17-98-1-8211, USPHS Grant No. CA 48129, and USAMRMC Grant No. DAMD 17-96-1-6254. The content of this publication does not necessarily reflect the position of the government, and no official endorsement of any equipment or product of any companies mentioned in the publication should be inferred.

[a]Electronic mail: chanhp@umich.edu

[1]S. A. Feig and R. E. Hendrick, ''Risk, Benefit, and Controversies in Mammographic Screening,'' in *Syllabus: A Categorical Course in Physics Technical Aspects of Breast Imaging,* edited by A. G. Haus and M. J. Yaffe (Radiological Society of North America, Oak Brook, IL, 1993).

[2]C. Byrne, C. R. Smart, C. Cherk, and W. H. Hartmann, ''Survival advantage differences by age: Evaluation of the extended follow-up of the Breast Cancer Detection Demonstration Project,'' Cancer (N.Y.) **74**, 301–310 (1994).

[3]Y. Wu, K. Doi, M. L. Geiger, and R. M. Nishikawa, ''Computerized detection of clustered microcalcifications in digital mammograms: Applications of artificial neural networks,'' Med. Phys. **19**, 555–560 (1992).

[4]H. P. Chan *et al.*, ''Improvement in radiologists' detection of clustered microcalcifications: The potential of computer-aided diagnosis,'' Invest. Radiol. **25**, 1102–1110 (1990).

[5]S. M. Lai, X. Li, and W. F. Bischof, ''On techniques for detecting circumscribed masses in mammograms,'' IEEE Trans. Med. Imaging **8**, 377–386 (1989).

[6]J. Kilday, F. Palmieri, and M. D. Fox, ''Classifying mammographic lesions using computerized image analysis,'' IEEE Trans. Med. Imaging **12**, 664–669 (1993).

[7]W. P. Kegelmeyer, J. M. Pruneda, P. D. Bourland, A. Hillis, M. W. Riggs, and M. L. Nipper, ''Computer-aided mammographic screening for spiculated lesions,'' Radiology **191**, 331–337 (1994).

[8]H. P. Chan, D. Wei, M. A. Helvie, B. Sahiner, N. Petrick, D. D. Adler, M. M. Goodsitt, and N. Petrick, ''Computer-aided classification of mammographic masses and normal tissue: Linear discriminant analysis in texture feature space,'' Phys. Med. Biol. **40**, 857–876 (1995).

[9]L. W. Bassett, B. Shayestehfar, and I. Hirbawi, ''Obtaining previous mammograms for comparison: Usefulness and costs,'' Am. J. Roentgenol. **163**, 1083–1086 (1994).

[10]E. A. Sickles, ''Periodic mammographic follow-up of probably benign lesions: Results in 3183 consecutive cases,'' Radiology **179**, 463–468 (1991).

[11] F. F. Yin, M. L. Giger, K. Doi, C. E. Metz, C. J. Vyborny, and R. A. Schmidt, ''Computerized detection of masses in digital mammograms: Analysis of bilateral subtraction images,'' Med. Phys. **18**, 955–963 (1991).
[12] F. F. Yin, M. L. Giger, K. Doi, C. J. Vyborny, and R. A. Schmidt, ''Computerized detection of masses in digital mammograms: Automated alignment of breast images and its effect on bilateral-subtraction technique,'' Med. Phys. **21**, 445–452 (1994).
[13] M. Sallam and K. Bowyer, ''Detecting abnormal densities in mammograms by comparison with previous screenings,'' in *Digital Mammography '96*, edited by K. Doi, M. L. Giger, R. M. Nishikawa, and R. A. Schmidt (Elsevier, Amsterdam, 1996).
[14] D. Brzakovic, N. Vujovic, M. Neskovic, P. Brzakovic, and K. Fogarty, ''Mammogram analysis by comparison with previous screenings'' in Ref. 13.
[15] N. Vujovic, D. Brzakovic, and K. Fogarty, ''Detection of cancerous changes in mammograms using intensity and texture measures,'' Proc. SPIE **2434**, 37–47 (1995).
[16] N. Vujovic, P. Bakic, and D. Brzakovic, ''Detection of potentially cancerous signs by mammogram followup,'' in Ref. 13.
[17] N. Vujovic and D. Brzakovic, ''Establishing the correspondence between control points in pairs of mammographic images,'' IEEE Trans. Image Process. **6**, 1388–1399 (1997).
[18] W. K. Zouras, M. L. Giger, P. Lu, D. E. Wolverton, C. J. Vyborny, and K. Doi, ''Investigation of a temporal subtraction scheme for computerized detection of breast masses in mammograms,'' in Ref. 13.
[19] A. R. Morton, ''Design of an x-ray beam equalization filter for mammographic imaging,'' M.S. thesis, Department of Environmental and Industrial Health, University of Michigan, 1996.
[20] A. R. Morton, H. P. Chan, and M. M. Goodsitt, ''Automated model-guided breast segmentation algorithm,'' Med. Phys. **23**, 1107–1108 (1996).
[21] A. J. Mendez, P. G. Tahoces, M. J. Lado, M. Souto, J. L. Correa, and J. J. Vidal, ''Automatic detection of breast border and nipple in digital mammograms,'' Comput. Methods Programs Biomed. **49**, 253–262 (1996).
[22] R. Chandrasekhar and Y. Attikiouzel, ''A simple method for automatically locating the nipple on mammograms,'' IEEE Trans. Med. Imaging **16**, 483–494 (1997).
[23] F. Maes, A. Collignon, D. Vandermeulen, G. Marchal, and P. Suetens, ''Multimodality image registration by maximization of mutual information,'' IEEE Trans. Med. Imaging **16**, 187–198 (1997).
[24] A. Maintz, E. Meijering, and M. Viergever, ''General multimodal elastic registration based on mutual information,'' Proc. SPIE **3338**, 144–154 (1998).
[25] N. Petrick, H. P. Chan, D. Wei, B. Sahiner, M. A. Helvie, and D. D. Adler, ''Automated detection of breast masses on mammograms using adaptive contrast enhancement and tissue classification,'' Med. Phys. **23**, 1685–1696 (1996).
[26] S. Sanjay-Gopal, H. P. Chan, B. Sahiner, N. Petrick, T. Wilson, and M. Helvie, ''Evaluation of interval change in mammographic features for computerized classification of malignant and benign masses,'' Radiology **205(P)**, 216 (1997).
[27] S. Sanjay-Gopal, H. P. Chan, N. Petrick, T. Wilson, B. Sahiner, M. Helvie, and M. Goodsitt, ''A regional registration technique for automated analysis of interval changes of breast lesions,'' Proc. SPIE **3338**, 118–131 (1998).